Neutron and x-ray scattering studies of the lightly doped spin–Peierls system $Cu_{1-x}Cd_xGeO_3$

2007 J. Phys.: Condens. Matter 19 436222

(http://iopscience.iop.org/0953-8984/19/43/436222)

IOP PUBLISHING JOURNAL OF PHYSICS: CONDENSED MATTER

J. Phys.: Condens. Matter **19** (2007) 436222 (12pp) doi:10.1088/0953-8984/19/43/436222

Neutron and x-ray scattering studies of the lightly doped spin–Peierls system $Cu_{1-x}Cd_xGeO_3$

S Haravifard[1], K C Rule[1], H A Dabkowska[1], B D Gaulin[1,2], Z Yamani[3] and W J L Buyers[2,3]

[1] Department of Physics and Astronomy, McMaster University, Hamilton, ON, L8S 4M1, Canada
[2] Canadian Institute for Advanced Research, 180 Dundas Street West, Toronto, ON, M5G 1Z8, Canada
[3] Canadian Neutron Beam Centre, NRC, Chalk River Laboratories, Chalk River, ON, K0J 1J0, Canada

E-mail: gaulin@mcmaster.ca

Received 6 July 2007, in final form 12 July 2007
Published 1 October 2007
Online at stacks.iop.org/JPhysCM/19/436222

Abstract

Single crystals of the lightly doped spin–Peierls system $Cu_{1-x}Cd_xGeO_3$ have been studied using bulk susceptibility, x-ray diffraction, and inelastic neutron scattering techniques. We investigate the triplet gap in the magnetic excitation spectrum of this quasi-one-dimensional quantum antiferromagnet, and its relation to the spin–Peierls dimerization order parameter. We employ two different theoretical forms to model the inelastic neutron scattering cross section and $\chi''(\mathbf{Q}, \omega)$, and show the sensitivity of the gap energy to the choice of $\chi''(\mathbf{Q}, \hbar\omega)$. We find that a finite gap exists at the spin–Peierls phase transition.

(Some figures in this article are in colour only in the electronic version)

1. Introduction

Low-dimensional quantum magnets [1] which display collective singlet ground states are very topical, due to the exotic low-temperature properties they display, as well as their relation to high-temperature superconductivity [2]. Quasi-two-dimensional $S = 1/2$ systems such as the Shastry–Sutherland system $SrCu_2(BO_3)_2$ exist [3–6], wherein orthogonal Cu^{2+} dimers are arranged on a square lattice. This material displays a collective singlet ground state, relatively dispersionless triplet excitations and multiple triplet bound excited states. Quasi-one-dimensional quantum magnets are more common, with $S = 1/2$ chains based on organic molecules, such as TTF-CuBDT [7, 8] and MEM-$(TCNQ)_2$ [9, 10], based on $Cu^{2+}(3d^9)$, such as $CuGeO_3$ [11–22], and most recently based on $Ti^{2+}(3d^1)$, such as TiOCl [23–25] and TiOBr [26]. These materials undergo spin–Peierls phase transitions to a singlet ground state as the temperature is lowered. Related phenomena occurs in quasi-one-dimensional quantum

magnets with $S = 1$ chains, such as NENP and $CsNiCl_3$ [27, 28], which enter a Haldane singlet phase at low temperatures.

$CuGeO_3$ was the first inorganic spin–Peierls system to be discovered. The singlet ground state associated with $CuGeO_3$ below its spin–Peierls phase transition temperature of $T_{SP} \sim 14.1$ K has been well studied [11–22]. Such a system is characterized by uniform chains of $S = 1/2$ moments at high temperatures, which dimerize at low temperature to allow singlets to form. This phase transition breaks translational symmetry, and a singlet–triplet gap is introduced into its magnetic excitation spectrum at its magnetic zone centre. It possesses a much higher magnetic moment density than the pre-existing organic spin–Peierls systems [7–10], and it can be grown in large single-crystal form by several different growth techniques. This has enabled detailed neutron scattering studies of the spin–Peierls ground state and its excitations [18]. $CuGeO_3$ can also be grown in the presence of impurities, and studies of doped $CuGeO_3$ have revealed the sensitivity of the spin–Peierls ground state to different types of impurities [11, 29]. In particular, they have revealed a remarkably rich temperature–impurity-concentration phase diagram in which antiferromagnetic long-range order coexists with either a dimerized or uniform structure at sufficiently low temperatures [31–38]. This occurs for both non-magnetic Zn^{2+} [31–34] and Mg^{2+} [38] substituting for Cu^{2+}, as well as for Si^{4+} [32, 35–37] substituting for Ge^{4+}.

Most of the work on impurities in $CuGeO_3$ has employed dopants which possess a similar or a smaller ionic radius than that of the host ion which they seek to replace. Zn^{2+}, Mg^{2+}, and Cu^{2+} have ionic radii of 0.74 Å, 0.66 Å, and 0.72 Å, respectively. However, some work has also been done on low-concentration substitution [29] of Cu^{2+} with Cd^{2+}, whose ionic radius is much bigger, 0.97 Å, than that of Cu^{2+}. The difference in ionic radii severely limits the solubility of Cd in $CuGeO_3$; nonetheless small single crystals of $Cu_{1-x}Cd_xGeO_3$ with $x \leqslant 0.002$ were grown and studied [29]. This previous study [29], on small single crystals grown from a flux, showed little change in T_{SP}, and no coexisting antiferromagnetism at the low Cd concentrations and base temperature that could be achieved. However, interestingly, the critical properties of the spin–Peierls phase transition changed from three-dimensional universality to mean-field behaviour on doping with Cd.

One interesting dimension of the spin–Peierls problem is the relation between the singlet–triplet gap in the spin excitation spectrum, and the order parameter for dimerization. Cross and Fisher [39] originally argued for the power-law relation $\Delta(T) \sim (\delta(T))^{\nu}$ with $\nu = 2/3$. The discovery of the spin–Peierls state in $CuGeO_3$ has allowed this relationship to be tested directly using inelastic and elastic neutron scattering to measure the temperature dependence of the gap energy, $\Delta(T)$, and the square of the order parameter for the spin–Peierls dimerization δ^2. We report here inelastic neutron scattering measurements of the temperature dependence of the magnetic excitation spectrum at the magnetic zone centre, and of the x-ray diffraction measurements of the superlattice Bragg peak intensity, in a new single crystal of lightly doped $Cu_{1-x}Cd_xGeO_3$ ($x \leqslant 0.002$). These results show that the simple power-law relation between the gap and the dimerization order parameter is not obeyed, and that a finite triplet gap exists at the spin–Peierls phase transition itself.

2. Experimental details

A single crystal of $Cu_{1-x}Cd_xGeO_3$ with $x \leqslant 0.002$ was grown by the self-flux method in a floating zone image furnace. The crystal was grown at a rate of ∼5–8 mm h^{-1} with an oxygen pressure of 47 kPa. Earlier experience [29] on flux-grown $Cu_{1-x}Cd_xGeO_3$ indicated a low solubility of Cd in the $CuGeO_3$ host. For that reason, naturally occurring Cd was used in the crystal growth, even though the crystals were intended for neutron scattering studies, and Cd

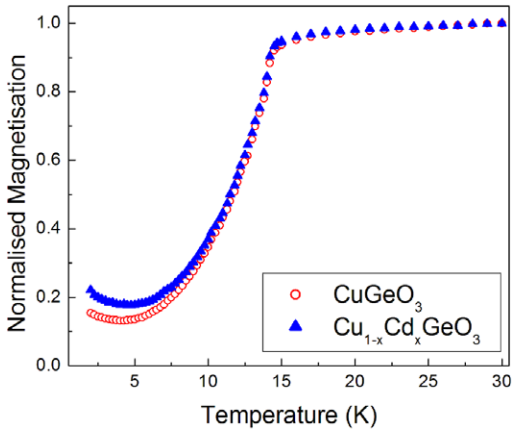

Figure 1. SQUID dc susceptibility measurements (with 1000 G applied magnetic field) on $CuGeO_3$ and $Cu_{1-x}Cd_xGeO_3$ with $x \leqslant 0.002$ are compared.

has a high neutron absorption cross section. Initial neutron diffraction measurements on the sample showed strong Bragg scattering, from a high-quality crystal that was single throughout its volume. Its approximate dimensions were of 30 mm length by 5 mm in diameter, and the mosaic spread was less than 0.4°. These measurements confirmed that the crystal was orthorhombic, with lattice parameters within error the same as those of the pure material: $a = 4.81$ Å, $b = 8.47$ Å and $c = 2.94$ Å at 4 K.

X-ray diffraction measurements were performed on a small single crystal cut from the large crystal used in the neutron scattering measurements. The crystal was mounted on the cold finger of a closed-cycle refrigerator and aligned within a Huber four-circle goniometer. The measurements with a rotating anode Cu Kα x-ray source and a pyrolytic graphite monochromator were performed at temperatures from 6.5 to 14.5 K with a temperature stability of ∼0.005 K. The primary purpose of these measurements was to precisely study the critical properties of the spin–Peierls order parameter, as measured by the temperature dependence of the $\mathbf{Q} = (\frac{1}{2}, 5, -\frac{1}{2})$ superlattice Bragg peak intensity, and to determine the critical exponent, β.

Another small piece of crystal was cut off and used for magnetic characterization with SQUID magnetometry. The characteristic falloff of the dc susceptibility signifying T_{SP} near 14.1 K was observed. Figure 1 shows the comparison of the normalized susceptibility measurement for both $CuGeO_3$ and $Cu_{1-x}Cd_xGeO_3$ samples as a function of temperature. It is clear from these data that the susceptibility of the doped sample is very similar to that of the pure material. At temperatures above T_{SP}, the susceptibility of both samples shows a broad maximum characteristic of short-range, quasi-one-dimensional correlations. Below 10 K, the $Cu_{1-x}Cd_xGeO_3$ susceptibility is ∼20% larger than that of the $CuGeO_3$ sample, indicating that Cd impurities are indeed present in the system. They have the effect of freeing up individual spins near the impurities, thereby increasing the susceptibility.

Elastic and inelastic neutron scattering measurements were performed on the large single crystal of $Cu_{1-x}Cd_xGeO_3$ at the Canadian Neutron Beam Centre, Chalk River, using the N5 triple-axis spectrometer. The crystal was mounted in a ^{3}He cryostat with its $(0, K, L)$ plane coincident with the horizontal scattering plane, such that wavevectors near the $\mathbf{Q} = (0, 1, \frac{1}{2})$ magnetic zone centre could be accessed. The measurements were made with pyrolytic graphite as both monochromator and analyser crystals, a fixed final neutron energy of

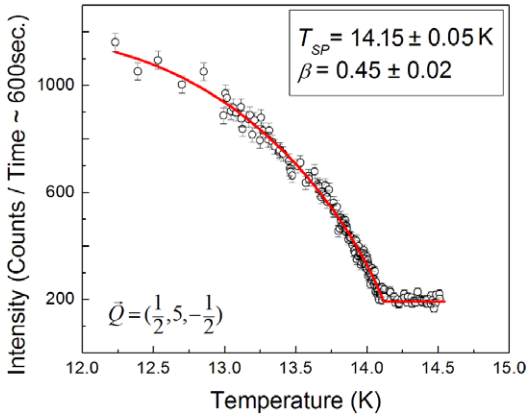

Figure 2. X-ray scattering measurements of the superlattice Bragg intensity at $\mathbf{Q} = (\frac{1}{2}, 5, -\frac{1}{2})$ are shown as a function of temperature. The solid line shows a fit of this temperature dependence to critical behaviour described in equation (1). We observe mean-field-like behaviour, consistent with earlier measurements on small flux-grown $Cu_{1-x}Cd_xGeO_3$ single crystals [29].

14.7 meV, and with two pyrolytic graphite filters in the scattered beam to reduce higher-order contamination. Soller slits determined the horizontal collimation and the resulting horizontal and vertical divergences of the beam were [38, 36, 36, 212] and [58, 73, 146, 636] respectively, in minutes of arc, using the convention [source–monochromator, monochromator–sample, sample–analyser, analyser–detector].

Elastic neutron scattering measurements were performed at the magnetic zone centre, $\mathbf{Q} = (0, 1, \frac{1}{2})$, to search for impurity-induced antiferromagnetic ordering at $T = 0.32$ K. No evidence for magnetic ordering was found.

The lack of change in T_{SP} in $Cu_{1-x}Cd_xGeO_3$ as compared with $CuGeO_3$, as well as the absence of magnetic order at $T = 0.32$ K, can be used to set an upper limit for the Cd concentration in the single-crystal sample of $Cu_{1-x}Cd_xGeO_3$. Assuming that the $Cu_{1-x}Mg_xGeO_3$ phase diagram [40] is applicable to $Cu_{1-x}Cd_xGeO_3$, at least at low doping concentrations, an upper limit of $x \leqslant 0.002$ can be set.

3. Experimental results and analysis

3.1. X-ray diffraction

We measured the temperature dependence of the $\mathbf{Q} = (\frac{1}{2}, 5, -\frac{1}{2})$ superlattice Bragg peak intensity, as shown in figure 2 for temperatures close to T_{SP}. This peak arises from the dimerization pattern within the spin–Peierls state in $CuGeO_3$, and its amplitude is proportional to the square of the order parameter.

As was done previously to examine the critical properties of doped $CuGeO_3$ [29], this peak intensity as a function of temperature was fitted to a modified power law as shown in equation (1). This modified power law includes a correction to scaling term [30], with the correction to scaling exponent η set to its expected value of 0.5 and $t = \frac{T_{SP}-T}{T_{SP}}$.

$$I = I_0 t^{2\beta} (1 + At^{\eta}) + \text{Background}. \tag{1}$$

The solid line in figure 2 shows the fit of equation (1) to the data, and clearly this expression describes the data very well for temperatures close to T_{SP}. The fit gives $T_{SP} = 14.15 \pm 0.05$ K and a critical exponent $\beta = 0.45 \pm 0.02$. This value is close to the mean-field value of $\beta = 0.5$,

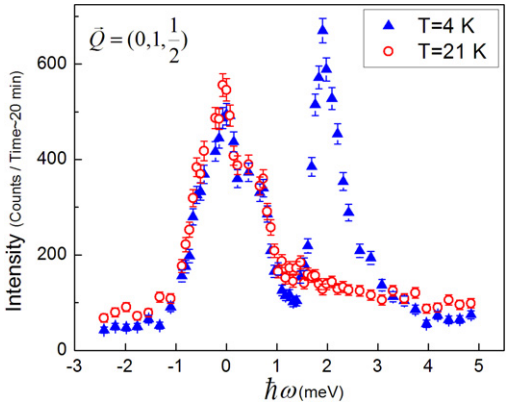

Figure 3. Constant-**Q** inelastic neutron scattering scans at the magnetic zone centre $\mathbf{Q} = (0, 1, \frac{1}{2})$, taken well below T_{SP} at $T = 4$ K and well above T_{SP} at $T = 21$ K.

and is much larger than the values for $\beta(\sim 0.33)$ from three-dimensional universality [41, 42] that are known to characterize both pure $CuGeO_3$ [19, 20] and lightly doped $CuGeO_3$ in which the dopants possess similar ionic radii to the host ions they replace [29].

This mean-field result is similar to that found by Lumsden *et al* [29] in which the critical behaviour of lightly doped single crystals of $Cu_{1-x}Cd_xGeO_3$ grown by the flux method also showed mean-field critical exponent β values. These results establish that some Cd impurities are present in the crystal, and also provide a quantitative form for the spin–Peierls order parameter as a function of temperature, which can then be compared to the temperature dependence of the triplet gap in the excitation spectrum obtained from inelastic neutron scattering.

3.2. Neutron scattering

Constant-**Q** inelastic neutron scattering scans were performed at the magnetic ordering wavevector $\mathbf{Q}_0 = (0, 1, \frac{1}{2})$ in order to observe the temperature dependence of the triplet excitations at the magnetic zone centre. The energies of the triplet excitations disperse with wavevector due to the three-dimensional nature of the magnetic system. Near the ordering wavevector, this dispersion [18] varies with the relative wavevector $\mathbf{q} = \mathbf{Q} - \mathbf{Q}_0$, as

$$\Delta_{\mathbf{q}} = \sqrt{\Delta^2 + (v_a q_a)^2 + (v_b q_b)^2 + (v_c q_c)^2} \tag{2}$$

where Δ is the minimum triplet excitation energy or gap energy. q_a, q_b and q_c are reduced wavevectors expressed in reciprocal lattice units, where

$$v_a q_a = (\Delta E)_a \sin(\pi q_a) \qquad \text{and} \qquad (\Delta E)_a \approx 1.66 \text{ meV}$$
$$v_b q_b = (\Delta E)_b \sin(\pi q_b/2) \qquad \text{and} \qquad (\Delta E)_b \approx 5.3 \text{ meV}$$
$$v_c q_c = c_0 q_c \qquad \text{and} \qquad c_0 = 80 \text{ meV}.$$

Representative data at 4 and 21 K, well below and well above T_{SP}, respectively, are shown in figure 3, and the low-temperature singlet–triplet gap of $\Delta \sim 2$ meV is identified in the 4 K data. At 21 K, the triplet excitation is completely absent and the finite-energy peak in the inelastic scattering has been replaced with a weak continuum of scattering from quasi-elastic energies, out to the end of the scan, 4.8 meV. We note that the triplet excitation at low temperatures exhibits an asymmetric tail to the high-energy side.

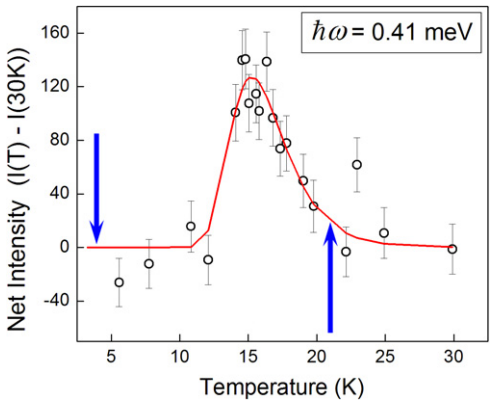

Figure 4. Net intensity of the neutron scattering observed at the magnetic zone centre, $\mathbf{Q} = (0, 1, \frac{1}{2})$ and an energy transfer of 0.42 meV is shown. The solid line is a guide to the eye and the vertical arrows indicate the temperatures at which the low-temperature and high-temperature background data sets were taken.

Figure 4 shows the temperature dependence of the quasi-elastic scattering at $\hbar\omega = 0.41$ meV and at $\mathbf{Q} = (0, 1, \frac{1}{2})$. It shows a 'critical' regime which extends from ∼12 to ∼21 K within which quasi-elastic scattering is significantly enhanced compared with either lower or higher temperatures. We wish to isolate the triplet excitation at $\mathbf{Q} = (0, 1, \frac{1}{2})$, from the incoherent elastic scattering as well as from the background scattering, and thereby determine the gap energy, Δ, as a function of temperature. This requires a background subtraction for which we have two options. We can use the low-temperature scattering at $T = 4$ K, suitably modified to exclude the resolution-limited triplet excitation, or we can use the scattering at 21 K. Each of these has advantages. For the $T = 4$ K data the triplet excitation is sharp in energy, and so can be cleanly separated from the remaining scattering, comprised of incoherent elastic scattering from the sample, and energy-independent background scattering from fast neutrons. However, the use of the $T = 4$ K data set as a background does not recognize that inelastic scattering persists above T_{SP}, albeit in the form of a weak, quasi-elastic spin excitation spectrum for which the $T = 21$ K data set is characteristic. In what follows, we employ both a suitably modified $T = 4$ K data set (LT background) as well as the $T = 21$ K data set (HT background) as the background data set to be subtracted from the signal so as to accurately estimate the scattering from the triplet excitation alone. This will allow us to examine the sensitivity of the gap, $\Delta(T)$, to the method of background scattering estimation.

Figure 5 shows representative constant-$\mathbf{Q}$ scans at $(0, 1, \frac{1}{2})$, for which a high-temperature or low-temperature data set has been subtracted from the scans at temperatures ranging from ∼0.7 T_{SP} (10 K) to ∼1.1 T_{SP} (15 K). This data was fitted to two different forms for $S(\mathbf{Q}, \omega)$ with the intention of determining the temperature dependence of the gap energy, Δ, and the inverse lifetime, Γ, of the triplet excitations. However, a qualitative examination of the data in figure 5 shows a substantial, well-defined inelastic peak to exist at ∼1.6 or ∼1.8 meV and $T = 13.83$ K ∼ 0.98 T_{SP}, depending on whether the low-temperature (LT) or high-temperature (HT) data set is used as a background. One would qualitatively conclude therefore that the gap remains finite at T_{SP} in this sample of $Cu_{1-x}Cd_xGeO_3$, a result that is borne out by a quantitative analysis of the excitation spectrum, discussed below.

The inelastic spectra, shown in figure 5, were fitted to two models of $S(\mathbf{Q}, \omega)$, each of which was convolved with the four-dimensional instrumental resolution function. The finite

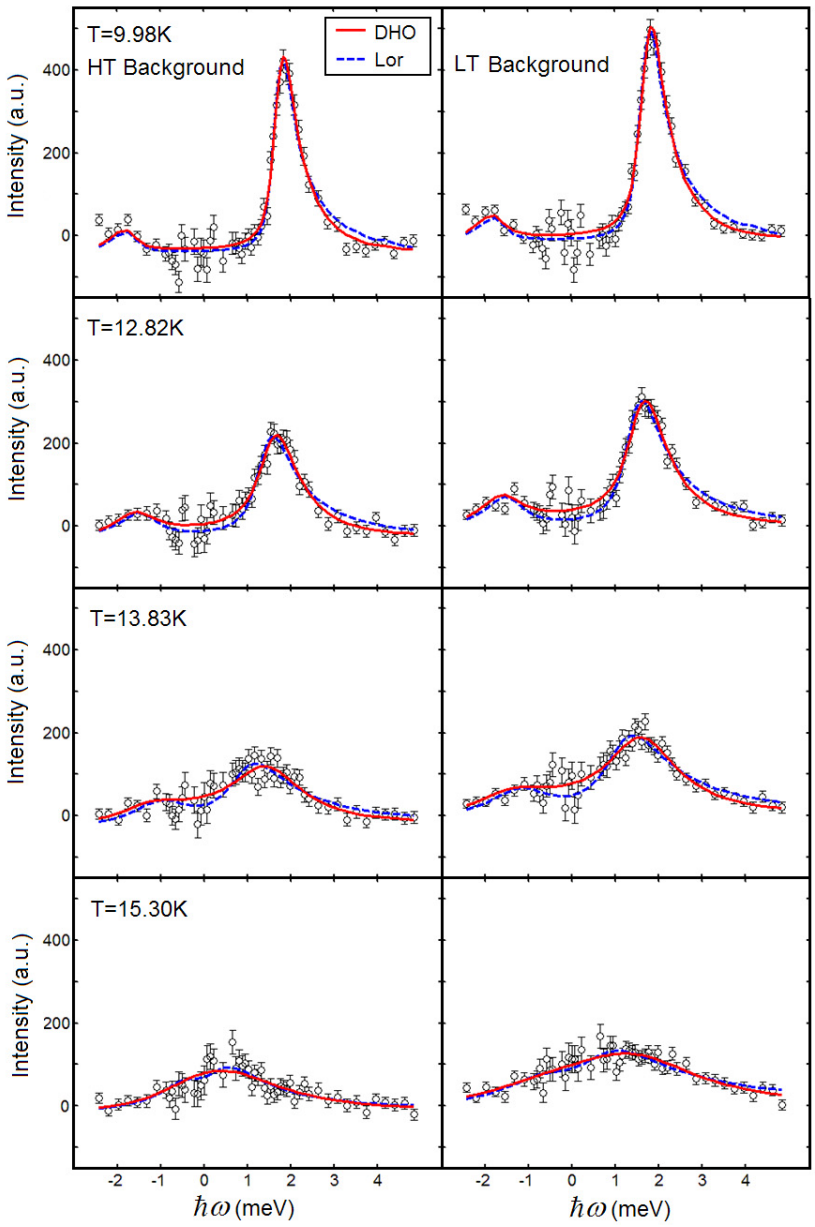

Figure 5. Representative inelastic spectrum, below and above $T_C = 14.15$ K, and at the magnetic zone centre $\mathbf{Q} = (0, 1, \frac{1}{2})$ are shown, using the high-temperature data set as background (left-hand panels), and the low-temperature data set as background (right-hand panels). The lines through the data show fits of the spectra to a Lorentzian and a damped harmonic oscillator (DHO) form of $S(\mathbf{Q}, \omega)$, as described by equations (3) and (4), respectively. The DHO model is clearly superior, especially at large energies.

resolution of the measurement combines with the dispersion of the triplet excitations to higher energies at wavevectors away from the magnetic zone centre, equation (2), and results in

the asymmetry of the triplet lineshape, with a high-energy tail. This is accounted for within our resolution convolution, where we employed the spin wave velocities (see equation (2)) determined previously [18].

The first Lorentzian model was employed by Regnault *et al* [18], in their analysis of the temperature dependence of the triplet excitation energy near the magnetic zone centre in pure $CuGeO_3$. The Lorentzian (Lor) profile is given by

$$S_{\mathrm{L}}(\mathbf{Q},\omega) \sim \frac{\omega}{1-\exp(-\omega/kT)}\left[\frac{\Gamma_{\mathrm{L}}}{(\omega-\Delta_{\mathrm{L}})^2+\Gamma_{\mathrm{L}}^2}+\frac{\Gamma_{\mathrm{L}}}{(\omega+\Delta_{\mathrm{L}})^2+\Gamma_{\mathrm{L}}^2}\right]. \quad (3)$$

The second model was a damped harmonic oscillator (DHO) given by

$$S_{\mathrm{D}}(\mathbf{Q},\omega) = \frac{\chi_0\Delta^2\pi^{-1}}{1-\exp(-\omega/kT)}\left[\frac{2\omega\Gamma}{(\omega^2-\Delta^2)^2+4\omega^2\Gamma^2}\right], \quad (4)$$

where χ_0 is the static susceptibility at $\mathbf{Q}$. For small damping, the relation between the gap energy in the DHO and Lor models is

$$\Delta_{\mathrm{L}}^2 = \Delta^2 - \Gamma^2. \quad (5)$$

The results of fitting the data to the Lor model and the DHO model are shown as the solid and dashed lines in figure 5. Both models are reasonable descriptors of the data. However, the DHO model is a better descriptor as its goodness-of-fit parameter, χ^2, is typically 10–40% lower than for the Lor model at all temperatures. This is because the Lor spectrum, used earlier [18], falls off too slowly with ω; indeed its integral in frequency is divergent. We conclude that the inelastic scattering is best described using the DHO form for $S(\mathbf{Q},\omega)$, equation (4).

The values of the gap energy, Δ, and inverse lifetime, Γ, of the triplet excitations extracted from this analysis are plotted as a function of temperature in figure 6. The top panel shows the parameters resulting from an analysis of the data using the HT background, while the bottom panel shows the parameters relevant to the LT background. As can be seen from figure 6, while the background data set used influences the details of the fit parameters, it does not affect the overall trends and general features of the temperature dependence of the gap and inverse lifetime of the triplet excitations.

4. Discussion

Our analysis, employing two different forms of $S(\mathbf{Q},\omega)$ and two different background subtractions, results in four forms of the gap energy, Δ, and inverse lifetime, Γ, as a function of temperature, which can then be compared with theoretical expectations. These are plotted as a function of temperature in figure 6, where the top panel shows the parameters arising from use of the HT background, and the bottom panel shows those arising from use of the LT background. As can be seen, the gap energy, $\Delta \sim 2$ meV at 4 K, is independent of both the form of $S(\mathbf{Q},\omega)$ and the details of the background, provided the lifetime of the triplets is sufficiently long, as it is below $T \sim 10$ K. Above ~10 K, differences between the fitted gap energies progressively increase as the energy width of the excitations, and hence the inverse lifetimes, become larger. However, in all four gap versus temperature plots shown in figure 6, the gap energy, Δ, does not appear to go to zero at $T_{\mathrm{SP}} \sim 14.15$ K. Rather, the phase transition occurs where the gap energy, Δ, and the energy width or inverse lifetime of the excitation, Γ, cross.

Figure 7 shows the gap energy, Δ, plotted as a function of the spin–Peierls order parameter as determined from the x-ray scattering determination of the temperature dependence of the superlattice Bragg peak intensity shown in figure 2. This net intensity is proportional to the

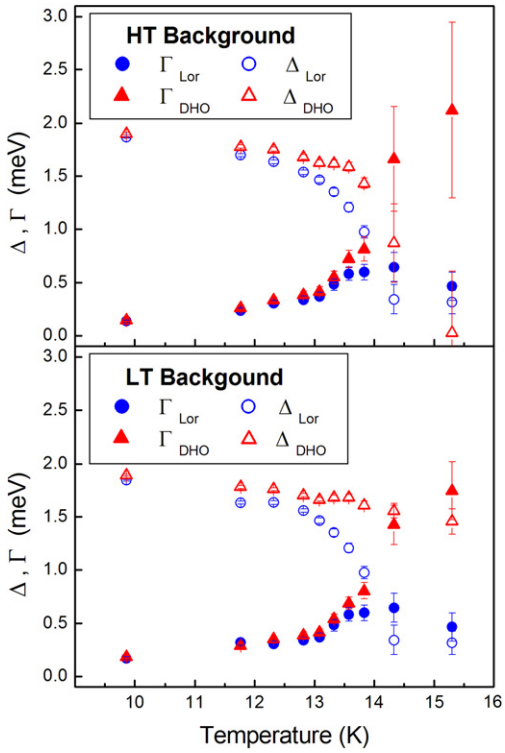

Figure 6. The temperature dependence of the energy gap, Δ, and inverse lifetime, Γ, of the triplet excitation is shown. The upper panel shows the fit parameters for both the Lorentzian and DHO models with the high-temperature background subtraction, while the lower panel shows the parameters extracted using the low-temperature background subtraction.

square of the order parameter, and consequently we have plotted the square root of the net intensity on the x-axis of figure 7. For reference, an x-axis label has been added to the top of figure 7 to denote the actual temperature. The top panel of figure 7 shows the analysis using the DHO form of $S(\mathbf{Q}, \omega)$, while the bottom panel shows that using the Lorentzian form.

The systematic dependence of the gap on the form of $S(\mathbf{Q}, \omega)$ and the details of the background can be seen in figures 6 and 7. As T_{SP} is approached, the DHO form of $S(\mathbf{Q}, \omega)$ produces a higher value of the gap energy as compared with the Lorentzian form. For either form of $S(\mathbf{Q}, \omega)$, the use of the LT background results in a higher gap energy near T_{SP}, as compared to when the HT background is used.

As previously discussed, theoretical expectations exist for the relation between the gap energy and the spin–Peierls order parameter: $\Delta(T) \sim \delta(T)^{\nu}$ with $\nu = \frac{2}{3}$. This argument was originally made by Cross and Fisher [39] in the context of the spin–Peierls transition in TTF-CuBDT [7, 8]. We have therefore fitted the data shown in figure 7 to $\Delta(T) = \Delta_0 + \delta(T)^{\nu}$, with Δ_0 a free parameter and also with Δ_0 set equal to zero. This latter case, with the gap going to zero at T_{SP}, is consistent with the original theoretical expectation [39]. The results of fitting our data to this expression are given in table 1, for all four data sets (DHO and Lor forms of $S(\mathbf{Q}, \omega)$, and both HT and LT backgrounds). As can be seen, the fits give a finite value of Δ_0, the gap energy at T_{SP}, unless it is constrained to be zero. Only one of the four combinations of $S(\mathbf{Q}, \omega)$ and background (Lor and HT background) give behaviour which is roughly consistent

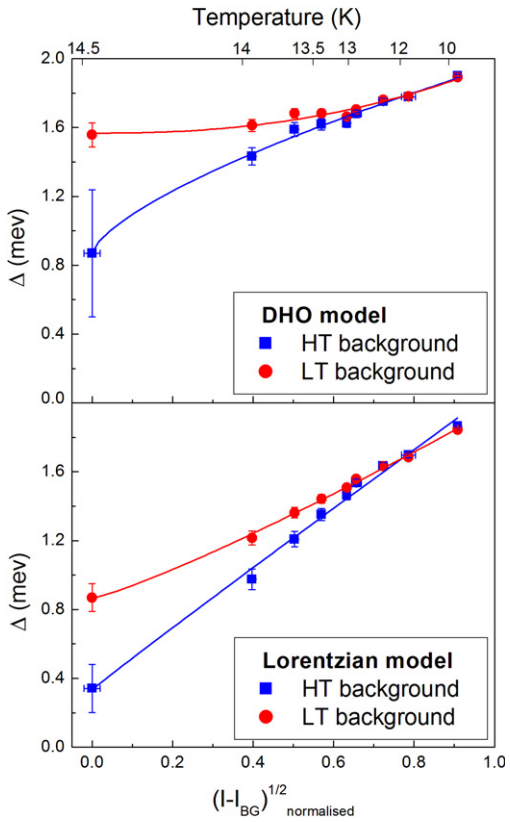

Figure 7. The gap energy, Δ, as a function of temperature is correlated with the corresponding spin–Peierls dimerization order parameter, taken as the square root of the net x-ray scattering intensity at the superlattice reflection $\mathbf{Q} = (\frac{1}{2}, 5, -\frac{1}{2})$. The upper panel shows the parameters resulting from the DHO form of $S(\mathbf{Q}, \omega)$, while the lower panel shows the parameters obtained from the Lorentzian form of $S(\mathbf{Q}, \omega)$. The lines in the figure are the results of fitting the data to $\Delta(T) = \Delta_0 + \delta(T)^{\nu}$, with Δ_0 a free parameter, and also with Δ_0 set equal to zero, as described in the text.

Table 1. Values of the exponent ν used to describe the power-law relationship between Δ and the order parameter.

	HT background		LT background	
	ν	Δ_0	ν	Δ_0
DHO	0.43 ± 0.06	0.85 ± 0.04	1.0 ± 0.4	1.54 ± 0.04
Lorentzian	0.67 ± 0.02	0.34 ± 0.02	0.82 ± 0.05	0.88 ± 0.02
DHO	0.30 ± 0.03	0	0.13 ± 0.03	0
Lorentzian	0.81 ± 0.04	0	0.48 ± 0.01	0

with $\Delta(T) \sim \delta(T)^{\nu}$ with $\nu = \frac{2}{3}$, and this case gives a finite gap at T_{SP} of 0.34 ± 0.02 meV. The fits using the DHO form of $S(\mathbf{Q}, \omega)$, which allows for the better-quality description of the inelastic neutron scattering spectra, give either very low values of the exponent ν, or non-zero values of the gap at T_{SP} ranging from ∼0.4 to 0.75× the zero-temperature value of the gap. We therefore conclude that the predicted relation $\Delta(T) \sim \delta(T)^{\nu}$ with $\nu = \frac{2}{3}$ is not obeyed in $Cu_{1-x}Cd_xGeO_3$, and that the gap is finite at T_{SP}.

A question arises as to what role doping plays in this behaviour. Systematic studies of the $Cu_{1-x}Mg_xGeO_3$ have shown a 'pseudogap' temperature regime to exist above T_{SP} for the low dopant concentrations which allow a spin–Peierls transition to occur [40]. This temperature regime is bordered from below by the appearance of long-range spin–Peierls order, and from above by signatures indicative of the presence of a gap, such as a suppression in the susceptibility. This pseudogap regime broadens in temperature with increasing doping until the spin–Peierls state is lost altogether beyond $x \sim 0.03$ in $Cu_{1-x}Mg_xGeO_3$. The low doping level present in the $Cu_{1-x}Cd_xGeO_3$ sample studied here, and the observation of pseudogap-like behaviour in $Cu_{1-x}Mg_xGeO_3$, suggest that the finite gap at T_{SP} may be intrinsic to pure $CuGeO_3$ as well. Surprisingly, in a previous study [18] the temperature dependence of $\Delta(T)$ for pure $CuGeO_3$ was found to be consistent with $\Delta(T) \sim \delta(T)^{\nu}$ with $\nu = \frac{2}{3}$. However, these earlier measurements focused on the triplet excitations at a wavevector slightly displaced from the dimerization zone centre, and employed the less satisfactory Lorentzian form for $S(\mathbf{Q}, \omega)$ only. Later measurements and analysis of the triplet excitations at the zone centre in pure $CuGeO_3$ were shown to be consistent with pseudogap behaviour [21, 22], that is a finite gap at T_{SP}, although a critical analysis testing the $\Delta(T) \sim \delta(T)^{\nu}$ relation was not performed.

It is notable that pseudo-gap behaviour has also been observed in the unconventional spin–Peierls material TiOCl [24, 25]. This material exhibits both a low-temperature dimerization into a singlet ground state below T_{SP1} and an intermediate temperature phase characterized by an incommensurate structural distortion. Above this phase transition, a uniform phase exists which displays characteristics of a finite gap, and the NMR signature for this pseudogap is maintained to $\sim$1.3 T_{SP2} [24].

5. Conclusions

Inelastic neutron scattering and x-ray diffraction measurements were carried out on a lightly doped sample of $Cu_{1-x}Cd_xGeO_3$. These x-ray diffraction measurements of the superlattice Bragg intensity below T_{SP} confirmed the mean-field behaviour of the spin–Peierls phase transition in this new large single crystal of $Cu_{1-x}Cd_xGeO_3$ grown by floating zone image furnace techniques. This result is consistent with earlier critical scattering measurements on small single crystals of $Cu_{1-x}Cd_xGeO_3$ grown by flux techniques [29].

The order parameter measurements as a function of temperature were correlated with inelastic neutron scattering measurements of the singlet–triplet energy gap in this singlet ground-state system, for the purpose of testing the relationship between the gap energy and the spin–Peierls order parameter. We investigated the sensitivity of the gap energy extracted from an analysis of the inelastic scattering to the form used to model $S(\mathbf{Q}, \omega)$ and to the form of the background scattering. This analysis showed the inelastic scattering to be best described using a DHO form for $S(\mathbf{Q}, \omega)$. We find that the energy gap remains finite at T_{SP}, as opposed to going to zero, as might have been anticipated on the basis of earlier theoretical expectations [39].

We hope that this result on lightly doped $Cu_{1-x}Cd_xGeO_3$ can inform and motivate further work on spin–Peierls and other singlet ground-state systems, and shed light on the formation of the triplet gap at and above T_{SP}.

Acknowledgments

We thank J E Lorenzo for drawing our attention to relevant literature. We acknowledge the expert technical assistance provided by the staff at NRC-CNBC, Chalk River. This work was supported by NSERC of Canada.

References

[1] See, for example: Skjeltorp A T and Sherrington D (ed) 1998 *Dynamical Properties of Unconventional Magnetic Systems* (*NATO ASI Series, Series E, Applied Sciences* vol 349) (Boston: Kluwer–Academic)
[2] See, for example: Orenstein J and Millis A J 2000 *Science* **288** 468
[3] Shastry B S and Sutherland B 1981 *Physica* B&C **108B** 1069
[4] Miyahara S and Ueda K 1999 *Phys. Rev. Lett.* **82** 3701
[5] Kageyama H, Yoshimura K, Stern R, Mushnikov N V, Onizuka K, Kato M, Kosuge K, Slichter C P, Goto T and Ueda Y 1999 *Phys. Rev. Lett.* **82** 3168
[6] Gaulin B D, Lee S H, Haravifard S, Castellan J P, Berlinsky A J, Dabkowska H A, Qiu Y and Copley J R D 2004 *Phys. Rev. Lett.* **93** 267202
[7] Bray J W, Hart H R, Interrante L V, Jacobs I S, Kasper J S, Watkins G D, Wee S H and Bonner J C 1975 *Phys. Rev. Lett.* **35** 744
[8] Jacobs I S, Bray J W, Hart H R, Interrante L V, Kasper J S, Watkins G D, Prober D E and Bonner J C 1976 *Phys. Rev.* B **14** 3036
[9] Huizinga S, Kommandeur J, Sawatzky G A, Thole B T, Kopinga K, de Jonge W J M and Roos J 1979 *Phys. Rev.* B **19** 4723
[10] Lumsden M D and Gaulin B D 1999 *Phys. Rev.* B **59** 9372
[11] Uchinokura K 2002 *J. Phys.: Condens. Matter* **14** R195
[12] Hase M, Terasaki I and Uchinokura K 1993 *Phys. Rev. Lett.* **70** 3651
[13] Hirota K, Cox D E, Lorenzo J E, Shirane G, Tranquada J M, Hase M, Uchinokura K, Kojima H, Shibuya Y and Tanaka I 1994 *Phys. Rev. Lett.* **73** 736
[14] Pouget J P, Regnault L P, Ain M, Hennion B, Renard J P, Veillet P, Dhalenne G and Revcolevschi A 1994 *Phys. Rev. Lett.* **72** 4037
[15] Kamimura O, Terauchi M, Tanaka M, Fujita O and Akimitsu J 1994 *J. Phys. Soc. Japan* **63** 2467
[16] Nishi M, Fujita O and Akimitsu J 1994 *Phys. Rev.* B **50** 6508
[17] Fujita O, Akimitsu J, Nishi M and Kakurai K 1995 *Phys. Rev. Lett.* **74** 1677
[18] Regnault L P, Ain M, Hennion B, Dhalenne G and Revcolevschi A 1996 *Phys. Rev.* B **53** 5579
[19] Lumsden M D, Gaulin B D and Dabkowska H A 1998 *Phys. Rev.* B **57** 14097
[20] Birgeneau R J, Kiryukhin V and Wang Y J 1999 *Phys. Rev.* B **60** 14097
[21] Lorenzo J E, Regnault L P, Langridge S, Vettier C, Sutter C, Grubel G, Souletie J, Lussier J G, Schoeffel J P, Pouget J P, Stunault A, Wermeille D, Dhalenne G and Revcolevschi A 1999 *Europhys. Lett.* **45** 45
[22] Lorenzo J E, Regnault L P, Hennion B, Ain M, Bourdarot F, Kulda J, Dhalenne G and Revcolevschi A 1997 *J. Phys.: Condens. Matter* **9** L211
[23] Seidel A, Marianetti C A, Chou F C, Ceder G and Lee P A 2003 *Phys. Rev.* B **67** 020405
[24] Imai T and Chou F C 2003 *Preprint* cond-mat/0301425
[25] Clancy J P, Gaulin B D, Rule K C, Castellan J P and Chou F C 2007 *Phys. Rev.* B **75** 100401(R)
[26] Sasaki T, Mizumaki M, Nagai T, Asaka T, Kato K, Takata M, Matsui Y and Akimitsu J 2005 *Preprint* cond-mat/0509358
[27] Ma S, Broholm C, Reich D H, Sternlieb B J and Erwin R W 1992 *Phys. Rev. Lett.* **69** 3571
[28] Buyers W J L, Morra R M, Armstrong R L, Hogan M J, Gerlach P and Hirakawa K 1986 *Phys. Rev. Lett.* **56** 371
[29] Lumsden M D, Gaulin B D and Dabkowska H A 1998 *Phys. Rev.* B **58** 12252 and references therein
[30] Aharony A and Ahlers G 1980 *Phys. Rev. Lett.* **44** 782
[31] Hase M, Terasaki I, Sasago Y, Uchinokura K and Obara H 1993 *Phys. Rev. Lett.* **71** 4059
[32] Oseroff S B, Cheong S-W, Aktas B, Hundley M F, Fisk Z and Rupp L W 1995 *Phys. Rev. Lett.* **74** 1450
[33] Lussier J-G, Coad S M, McMorrow D F and Paul D McK 1995 *J. Phys.: Condens. Matter* **7** L325
[34] Sasgo Y, Koide N, Uchinokura K, Martin M C, Hase M, Hirota K and Shirane G 1996 *Phys. Rev.* B **54** R6835
[35] Renard J P, Le Dang K, Vellet P, Dhalenne G, Revcolevschi A and Regnault L P 1995 *Europhys. Lett.* **30** 475
[36] Regnault L P, Renard J P, Dhalenne G and Revcolevschi A 1995 *Europhys. Lett.* **32** 579
[37] Poirier M, Beaudry R, Castonguay M, Plumer M L, Quirion G, Razavi F S, Revcolevschi A and Dhalenne G 1995 *Phys. Rev.* B **52** R6971
[38] Masuda T, Fujioka A, Uchiyama Y, Tsukada I and Uchinokura K 1998 *Phys. Rev. Lett.* **80** 4566
[39] Cross M C and Fisher D S 1979 *Phys. Rev.* B **19** 402
[40] Nishi M, Nakao H, Fujii Y, Masuda T, Uchinokura K and Shirane G 2000 *J. Phys. Soc. Japan* **69** 3186
[41] Collins M F 1989 *Magnetic Critical Scattering* (New York: Oxford University Press)
[42] Newman K G and Riedel E K 1982 *Phys. Rev.* B **25** 264